Journal of Applied Physics | ARTICLE | scitation.org/journal/jap

Annealing-temperature-dependent evolution of hydrogen-related donor and its strong correlation with *X*-photoluminescence center in proton-irradiated silicon

Cite as: J. Appl. Phys. **131**, 125702 (2022); doi: 10.1063/5.0083249
Submitted: 23 December 2021 · Accepted: 7 March 2022 ·
Published Online: 22 March 2022

View Online Export Citation CrossMark

Akira Kiyoi,[1,2,a)] Naoyuki Kawabata,[1] Katsumi Nakamura,[3] and Yasufumi Fujiwara[2]

AFFILIATIONS

[1]Advanced Technology R&D Center, Mitsubishi Electric Corporation, 8-1-1 Tukaguchi-Honmachi, Amagasaki, Hyogo 661-8661, Japan
[2]Division of Materials and Manufacturing Science, Graduate School of Engineering, Osaka University, 2-1 Yamadaoka, Suita, Osaka 565-0871, Japan
[3]Power Device Works, Mitsubishi Electric Corporation, 1-1-1 Imajuku-Higashi, Nishi-ku, Fukuoka, Fukuoka 819-0192, Japan

[a)]**Author to whom correspondence should be addressed:** Kiyoi.Akira@ay.MitsubishiElectric.co.jp

ABSTRACT

We have investigated the formation and decay of hydrogen-related donors (HDs) and irradiation-induced intrinsic defects. *N*-type m:Cz and FZ silicon wafers, which were irradiated with 2 MeV protons and subsequently annealed at 100–600 °C, were analyzed using spreading resistance profiling and photoluminescence (PL). HDs formed at 260 °C and then disappeared in two stages at 400–440 and 500–540 °C. This decay behavior indicates the existence of two types of HDs with different thermal stabilities. PL measurements showed interstitial silicon clusters (*W* and *X* center), a carbon–oxygen complex (*C* center), and exciton lines bound to unknown shallow centers. The origin of the HDs was investigated based on the correlation of the formation and decay temperatures between HDs and irradiation-induced defects. The predominant defects at the early stage of annealing, such as the *C* and *W* centers, are ruled out as candidates for the core defects of HDs because annealing above 260 °C is indispensable for the HD formation. In contrast, the *X* center was found to be thermally generated above 200 °C and disappeared at 580 °C. The similarity of the formation and decay temperatures between the *X* and HD centers suggests that HDs are associated with the formation of the interstitial silicon-related defects attached to hydrogen. Our results suggest that controlling the formation of interstitial silicon-related defects is important for realizing desirable doping profiles with high accuracy and reproducibility for power devices. Annealing above 400 °C exclusively provides thermally more stable HDs, leading to the realization of more rugged power devices.

Published under an exclusive license by AIP Publishing. https://doi.org/10.1063/5.0083249

I. INTRODUCTION

It is known that proton irradiation and subsequent annealing at moderate temperature induce shallow donor defects.[1,2] This doping method is prominent in modern power devices with wide field-stop layers because the large penetration depth of proton into silicon is suitable for the fabrication of thick *n*-type regions in the depth of silicon wafers, while the penetration depth in the conventional implantation of the group V element is limited to several micrometers.[3–5] The proton-irradiation-induced donors have been phenomenologically speculated to be defect complexes containing hydrogen and called hydrogen-related donors (HDs). Similar donor states were also observed in silicon irradiated with neutron,[6] electron,[7–9] helium ion,[10,11] and proton.[12–21] Therefore, it has widely been recognized that the core of HDs evolves from crystal damage. Additionally, when sufficient hydrogen is available, it may partially terminate the dangling bonds of irradiation-induced defects to generate donor states in silicon. Infrared electronic absorption studies have revealed the existence of a group of donor

Published under an exclusive license by AIP Publishing

states with ionization energies in the range of 34–53 meV and the incorporation of hydrogen in HDs through the shift of the absorption line in deuterated silicon.[6,8] Based on experimental results and *ab initio* density functional theory (DFT) calculations, the atomic structures of HDs have also been studied. It has been suggested that oxygen-related defects (vacancy-oxygen complex [VO][8,9] and interstitial carbon-interstitial oxygen complex [C_iO_i][22,23]) are associated with the formation of HDs. It has also been reported that HDs are related to intrinsic defects (vacancies and interstitial silicon and their clusters).[12,16–19] Gorelkinskii *et al.*[16] suggested that interstitial silicon-related defects participated in the HD formation process. Their electron paramagnetic resonance (EPR) results showed that the HD center had a large atomic reorientation energy (2.3 eV) comparable to typical intrinsic defect clusters such as tetra-interstitial Si. Tokmoldin and Mukashev[18,19] reported that Si–H bond stretching modes originate from the interstitial Si-hydrogen complex in proton-irradiated FZ silicon and associated this interstitial Si-hydrogen complex with HD. We have recently reported that HD concentration showed linear increasing dependence with proton-irradiation dose at 300–400 °C but was less dependent on oxygen concentration in silicon wafers.[21] Based on these results, we have proposed that the incorporation of interstitial silicon-related defects rather than oxygen-related defects in the formation of HDs is highly probable.

The annealing kinetics of HDs have been investigated previously.[9,13] Furthermore, the existence of several HD species has been demonstrated, but no investigation has been done concerning the correlation of the formation and decay temperatures between HDs and interstitial silicon-related defects. In the present study, we irradiated *n*-type m:CZ and FZ silicon wafers with 2 MeV protons and subsequently annealed them at 100–600 °C and investigated the annealing-temperature dependence of the HD concentration and irradiation-induced defects using spreading resistance (SR) profiling and photoluminescence (PL) techniques. We discussed the formation and decay processes of HDs and irradiation-induced defects to reveal the constituent defects of HDs. In our opinion, the physical mechanisms leading to HD formation should be clarified to realize desirable doping profiles with high accuracy and reproducibility, using different types of silicon wafers in the development of power devices as well as through the progress of hydrogen-related silicon technology.

II. EXPERIMENT

We used (100)-oriented phosphorus-doped *n*-type m:Cz and FZ silicon wafers. Phosphorus concentrations were 1.6×10^{14} and 2.0×10^{14} cm^{-3}, respectively. Carbon concentrations were 1.1×10^{15} and 2.0×10^{15} cm^{-3}, respectively. Oxygen concentrations were 1.8×10^{17} and 9.9×10^{15} cm^{-3}, respectively.

The wafers were irradiated with 2 MeV protons using a cyclotron particle accelerator (CYPRIS-370V, Sumitomo Heavy Industry, Ltd., Japan). At this acceleration energy, according to the SRIM2013 simulation program,[24] the depth of the projected ion ranges (R_p) was calculated to be 44.5 μm from the incident surface. The total irradiation dose was set to 1×10^{14} cm^{-2}. The irradiation was performed intermittently at sufficiently low beam currents to avoid unintentional annealing during irradiation. This procedure guaranteed sample temperatures below 150 °C.

After the irradiation, the wafers were cut into a suitable size ($5 \times 5 \times 0.73$ mm^3) and annealed at 100–600 °C for 1 h in an oven in atmospheric air. The annealing temperature was controlled using a temperature controller equipped with a thermocouple placed close to the sample. After the annealing, the samples were removed from the oven and immediately immersed in water to bring them to room temperature (~25 °C).

Two-point SR profiling measurements were performed at approximately 25 °C using an SR profiler (SSM-2000, Solid State Measurements, Inc., USA) with a bevel angle of 2.5° to achieve an adequate depth resolution of 0.25 μm. The measured SR profiles were transformed into equivalent carrier concentration profiles via the calibration with a standard (100) silicon wafer, assuming that all regions exhibited *n*-type conductivity.

PL measurements were performed at 20 K under excitation of the 633-nm line of a He-Ne laser with a beam diameter of approximately 1.6 μm and an incident power of 0.8 mW at a cryostat window using a PL spectrometer (HR-800, Horiba Jobin Yvon, Ltd., Japan). The samples were mounted on a closed-cycle cryostat for low-temperature measurements. Emissions from the samples were dispersed by using a monochromator with a 150 grooves/mm grating, blazed at 1.1 μm, and detected by an InGaAs photodiode array with a spectral resolution of 0.83 nm (0.85 meV). In the PL measurements, we used the same samples as those that were measured via SR profiling; the excitation laser was focused on the beveled surfaces of the samples. In this manner, the area corresponding to the depth around R_p was selected.

III. RESULTS AND DISCUSSION

A. HD formation and decay

To investigate the formation and decay of proton-irradiation-induced HDs, we compared the SR profiles of silicon wafers irradiated with 2 MeV protons and subsequently annealed at different temperatures in the range of 100–600 °C and an increment of 20 °C. Figure 1 shows the carrier concentration profiles of the m:Cz and FZ samples annealed at respective temperatures for 1 h. The carrier concentration profiles of the as-irradiated samples are also shown in Fig. 1, together with the profiles of the primary defect and hydrogen concentration, calculated by SRIM[24] with detailed calculations with full damage cascades. At 200 °C, the carrier compensation effect induced by irradiation-induced shallow acceptor defects led to a reduction in the carrier concentration across the proton-penetrated region. After annealing above 260 °C, broad peaks of the carrier concentration appeared around R_p in both wafers. These peaks corresponded to the *n*-type region where the shallow HD centers were induced due to the reaction between the implanted hydrogen and the irradiation-induced defects. We focused on these broad peaks to discuss the annealing-temperature dependence of the HD formation and decay. The concentration of the HD peaks increased with the increasing annealing temperature up to 340 °C, accompanied by the peak broadening that was a result of the diffusion of implanted hydrogen and the reaction with defects lying across the proton-penetrated region.

Published under an exclusive license by AIP Publishing

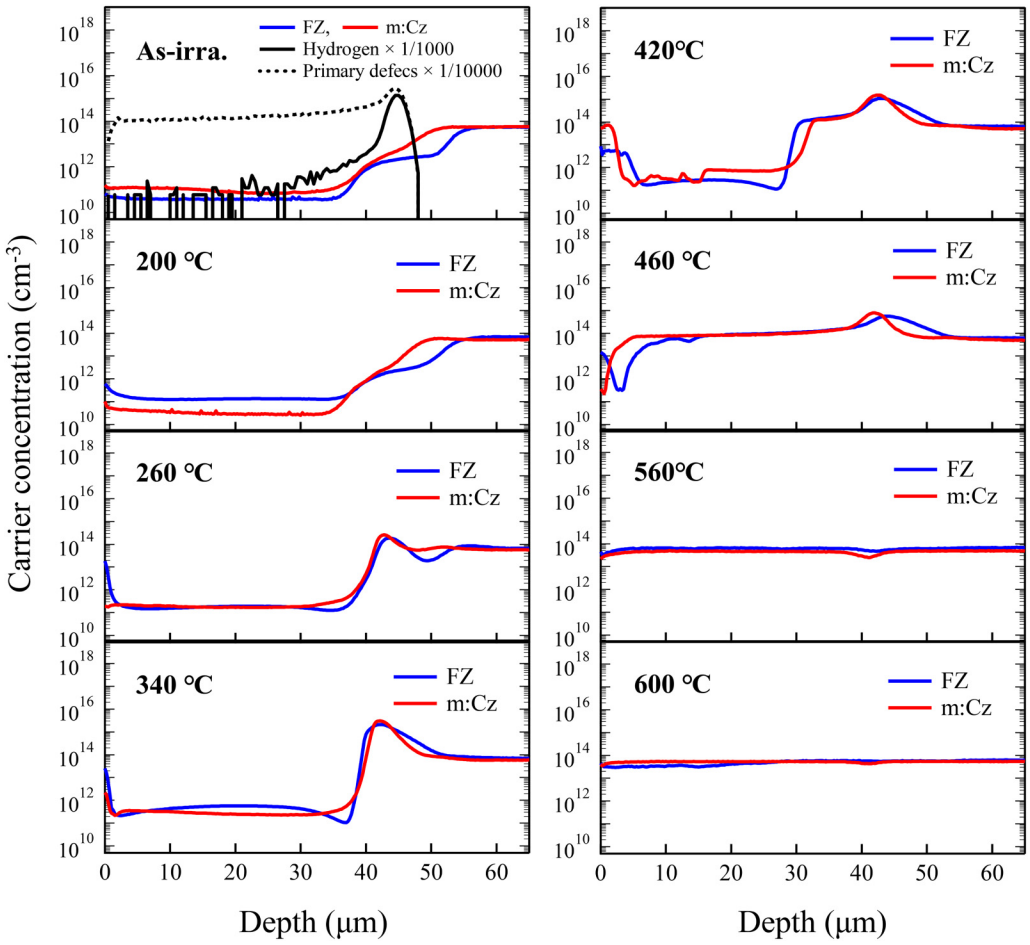

FIG. 1. Carrier concentration profiles of m:Cz and FZ samples irradiated with 2 MeV protons at a dose of 1×10^{14} cm^{-2} and subsequently annealed at a temperature range of 100–600 °C for 1 h. The profiles of the primary defect and hydrogen concentration, calculated by SRIM, are also shown for comparison with the carrier profiles in as-irradiated samples.

The HDs partially decayed above 340 °C and completely disappeared at 560 °C where a small dip due to residual shallow acceptor defects remained around R_p.

In addition, at the temperature range between 260 and 460 °C, the type conversion from *n*-type to *p*-type occurred in the FZ wafer, due to acceptor-type defects. Consequently, *p-n* junctions were observed (e.g., the dips at a depth of 37 μm for 340 °C in Fig. 1). On the contrary, the m:Cz wafer did not show any sign of *p-n* junctions, probably due to an additional thermal donor formation, which compensated the acceptor defects.[20] The *p-n* junction shifted as increasing the annealing temperature due to the hydrogen diffusion and subsequent HD formation through the penetrated layers.

Figure 2 shows the maximum and integrated HD concentrations of the m:Cz and FZ samples as a function of the annealing temperature. The maximum HD concentration was considered as the value of the peak near R_p and the integrated concentration was calculated as the sum of the carrier concentration in the depth direction of the wafer, across which the observed carrier concentration exceeded the original bulk carrier concentration of each wafer. The calibration procedure was used to extract the net HD concentration in the same manner as described in Ref. 21. (The net HD concentration was estimated as the carrier concentration of the annealed samples minus that of the as-irradiated sample, in which the HD centers did not form.) The peaks of the maximum HD concentration were observed at 340 °C regardless of the wafer type, but the maximum HD concentration of m:Cz silicon was 1.5 times higher than that of FZ silicon, whereas the integrated concentrations of both wafers were comparable at all annealing temperatures. This result indicates that the HDs existing around R_p acted as a reservoir of hydrogen in the early stage of the annealing process up to 340 °C. They thermally released hydrogen upon annealing, and the migrating hydrogen was captured by certain defects to form other HDs in the proton penetrated region. This phenomenon led to the

Published under an exclusive license by AIP Publishing

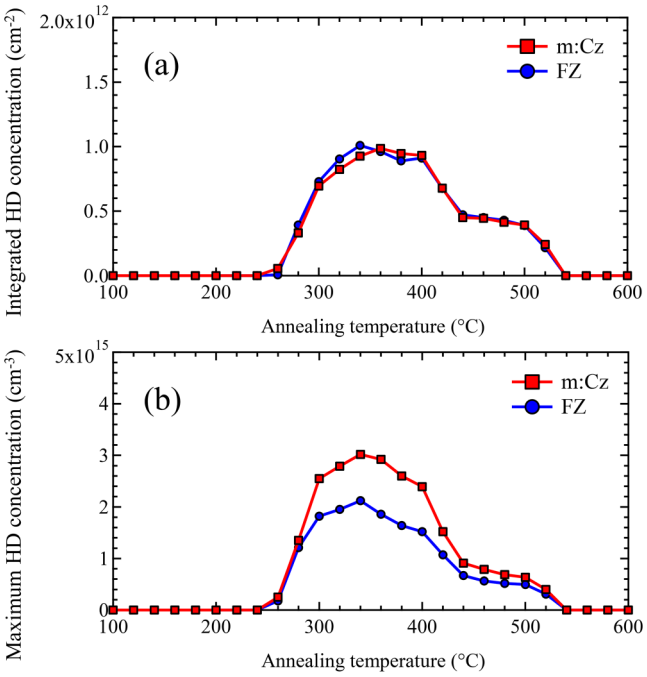

FIG. 2. Annealing-temperature dependence of the HD concentration. (a) Integrated and (b) maximum HD concentrations defined in the text. The squares and circles correspond to m:Cz and FZ samples, respectively. The annealing duration of the respective temperatures was 1 h. The solid lines are shown solely to facilitate visualization.

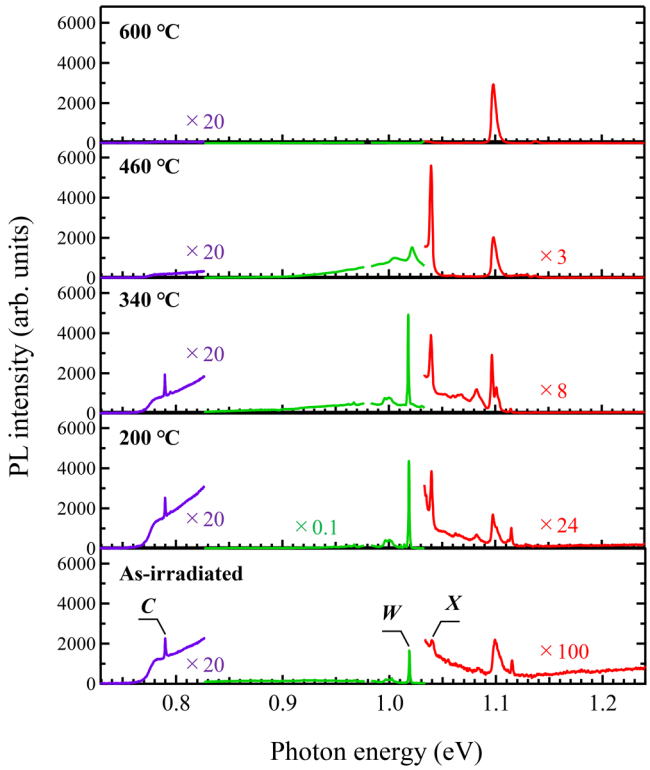

FIG. 3. PL spectra of m:Cz samples irradiated with 2 MeV protons and subsequently annealed at 200, 340, 460, and 600 °C for 1 h. *X*, *W*, and *C* denote the defect-related lines described in the text.

preservation of the integrated HD concentration, while the maximum HD concentration around R_p decreased as the annealing temperature increased. In addition, we recently reported that oxygen-related defects preferentially trapped hydrogen.[20] This trap-limited diffusion nature of hydrogen may result in the difference of the maximum HD concentration between m:Cz and FZ silicon.

In contrast, the integrated and maximum HD concentrations showed the same decreasing profiles as the annealing temperature increased in the m:Cz and FZ wafers. The first decay of the HDs appeared at 400–440 °C, and the second decay appeared at 500–540 °C. This behavior suggests the existence of at least two types of HD centers that have different thermal stabilities, consistent with previous studies.[9,13,20] It was assumed that the thermal decay was induced by either the dissociation of HDs or the passivation of dangling bonds of defects[25] consisting of HDs, in which the passivation led to the deactivation of the shallow donor states of HDs. In Ref. 20, based on the decay curves of HD concentration measured at 350–400 °C, we reported an activation energy of 1.9 eV for the first decay process of HDs. At 600 °C, the HDs completely disappeared, and the carrier profiles recovered to the original silicon wafers in the m:Cz and FZ wafers. In the application respect, this temperature dependence of HD concentration suggests that annealing at approximately 360 °C results in the highest concentration of HDs, leading to the most effective doping activation factor preferred in the cost-effective fabrication process of power devices. In contrast, annealing above 400 °C exclusively provides thermally more stable HDs, leading to the realization of more rugged power devices.

B. Defect formation and decay

We performed PL measurements on the same samples measured via SR profiling. The excitation laser was focused on the area on the bevel, corresponding to the depth around R_p for investigating the irradiation-induced defects existing in the regions where most implanted hydrogen atoms exist. Figure 3 shows the PL spectra of the m:Cz samples annealed at four temperatures in the range of 100–600 °C for 1 h. The *C* line and the *W* line, with zero-phonon lines (ZPLs) at 789.5 and 1018 meV, appeared immediately after irradiation.

It is well-known that an interstitial Si induced by irradiation reacts with a substitutional carbon atom C_s to generate an interstitial carbon C_i that immediately couples with an interstitial oxygen O_i to form a *C* center.[26–28] In addition to the reaction with carbon atoms, the clustering of interstitial Si is generated because single interstitial Si is highly mobile at room temperature[29] and damage events condense around R_p during proton irradiation. The *W* center

Published under an exclusive license by AIP Publishing

TABLE I. Photon energies of the ZPLs, proposed origins, and electronic levels of the observed PL lines.

Line	ZPL (meV)	Origin proposed in early studies	
		Defect	Electronic level (eV)
C	789.5	C_iO_i[27]	(0/+) E_v +0.38[27]
W	1018.2	Tri-interstitial Si[33–35]	(0/+) E_v +0.1,[34] E_v +0.19[33]
X	1039.8	Tetra-interstitial Si[33–35,37]	(0/+) E_v +0.29,[33] E_v +0.27[38]

is an interstitial Si cluster linked to the paramagnetic *B*5 center with trigonal symmetry[30] and is suggested to be monointerstitial,[31] di-interstitial,[32] and tetra-interstitial.[33–36] The ZPL of the *X* center (1039.5 meV) was also observed above 200 °C and it gradually increased in intensity up to 460 °C. The *X* center is linked to the *B*3 paramagnetic center with tetragonal symmetry and is identified as a tetra-interstitial[33–37] based on the discussion of the ^{29}Si hyperfine structure.[37] Some of the observed PL lines, well discussed in early studies, are summarized in Table I.

Figure 4 shows the high-energy regions of the PL spectra for the samples annealed at 200, 340, and 460 °C. In both the m:Cz and FZ samples, eight PL lines (at 1082, 1097, 1101, 1106, 1114, 1124, 1130, and 1137 meV, shown with arrows in Fig. 4) were observed near the energy gap of silicon at 200–460 °C. Similar PL lines have previously been reported as isoelectronic luminescence centers such as *B* defect[39,40] and *J*-line defect.[41] *Ab initio* DFT calculations demonstrated that the *B* defect (B_{41} and B^1_{71}) and *J*-line defect were linked with hexa-vacancy-hydrogen complexes (V_6H) and V_6 with shallow acceptor states;[42] however, a satisfactory explanation does not exist regarding the origin of these PL lines. Excitation power dependence measurements showed no blue shift of the lines for the observed PL lines (Fig. 5). Concurrently, the sample temperature dependence of PL intensity showed the disappearance of lines above 40 K (Fig. 6), suggesting a larger binding energy of the bound excitons than that of substitutional phosphorus atoms. Therefore, these lines are assumed to be due to excitons bound to unknown shallow defects with a structure similar to that of (V_6H) rather than due to donor–acceptor pair luminescence, including HDs (it is considered that HDs, phosphorus donors, and irradiation-induced acceptors coexisted in our samples).

Figure 7 shows the intensity of the *X*, *W*, *C*, and 1114-meV lines as a function of the annealing temperature. The intensity of the 1114-meV line (indicated as 5 in Fig. 4), which was the most discriminable among the eight lines, is plotted as the representative of the unknown bound excitons. The intensity of the *W* line increased up to 220 °C and decreased sharply at 440 °C. In contrast, the intensity of the *X* line gradually increased up to 460 °C and decreased at 580 °C. The decrease of the *W* line accompanied a slight increase of the *X* line, but the low-temperature annealing up to 220 °C apparently indicated that the generation of the *X* center proceeded concurrently with the generation of the *W* center. Therefore, the decrease of the *W* center was not the main reason behind the formation of the *X* center. The intensities of the *W* and

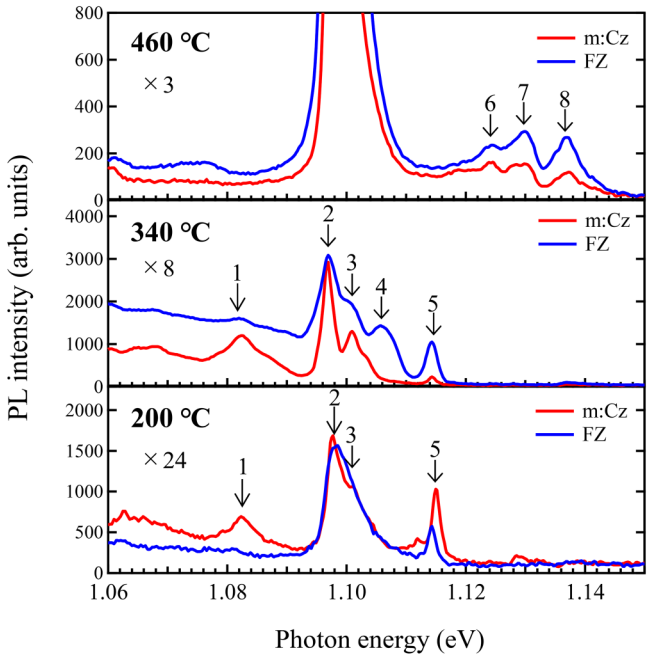

FIG. 4. High-energy regions of the PL spectra of m:Cz and FZ samples irradiated with 2 MeV protons and subsequently annealed at 200, 340, and 460 °C. The red and blue lines denote the spectra of the m:Cz and FZ samples, respectively.

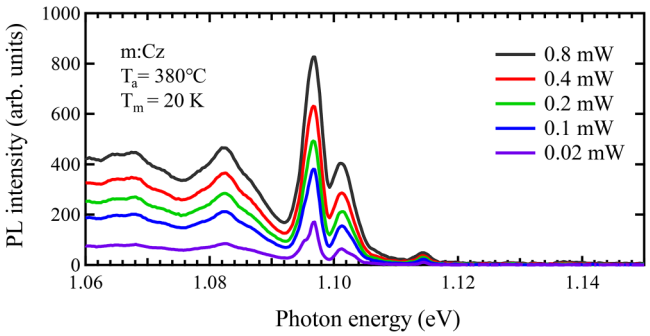

FIG. 5. PL spectra of m:Cz samples irradiated with 2 MeV protons and subsequently annealed at 380 °C, measured at different excitation powers ranging from 0.02 to 0.8 mW at a sample temperature of 20 K. PL was not detected at low excitation powers below 0.02 mW.

Published under an exclusive license by AIP Publishing

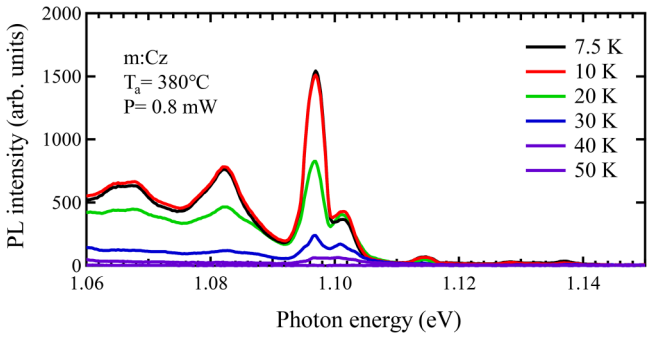

FIG. 6. PL spectra of m:Cz samples irradiated with 2 MeV protons and subsequently annealed at 380 °C, measured at different sample temperatures ranging from 7.5 to 50 K with an excitation laser power of 0.8 mW.

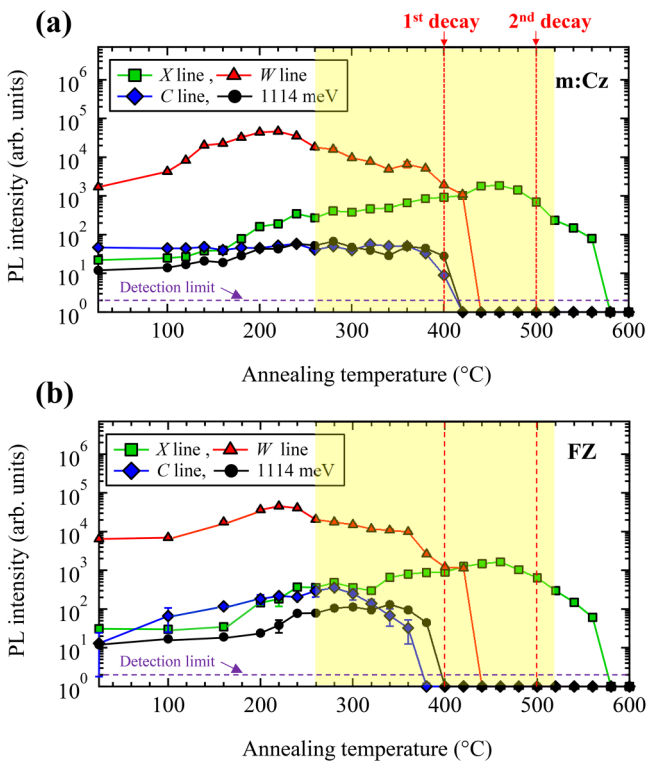

FIG. 7. Intensities of the PL lines as a function of the annealing temperature observed in (a) m:Cz and (b) FZ samples. The squares, triangles, and diamonds correspond to the *X*, *W*, and *C* lines, respectively. The circles also represent the intensity of the 1114-meV line described in the text. The standard deviations of some data points are shown by error bars, but most data points have deviations corresponding to the heights of the symbols. The solid lines are shown solely to facilitate visualization. The temperature range where HDs were observed and the temperatures at which the decay of HDs started are indicated with the yellow-filled area and red broken lines, respectively, for a comparison of the formation and decay temperatures between HDs and irradiation-induced defects.

X lines were independent of the wafer type. This trend is consistent with the fact that the *W* center and the *X* center are related to intrinsic defects.[33–37] Conversely, the *C* line was stable up to 360 °C in the m:Cz silicon, whereas an increasing tendency appeared in the FZ silicon. This discrepancy was presumably due to the encounter rate of mobile C_i with a stable O_i. The FZ wafer was relatively oxygen-lean; therefore, the long-range diffusion of C_i was necessary to make C_i encounter O_i adequately. The *C* center disappeared at approximately 400 °C, regardless of the wafer type.

As discussed in Sec. III A, the HD formation was unobservable in the as-irradiated stage; nevertheless, hydrogen and defects coexisted in the region near R_p upon proton irradiation. The HDs grew with subsequent annealing at higher temperatures above 260 °C. This fact suggests that the core defects consisting of HDs were generated during the annealing stage, and the reaction between hydrogen and the core defects proceeded concurrently with the generation of the core defects. Therefore, we ruled out C_iO_i and the *W* center, which were predominant at the early annealing stage, as candidates of the core defects of HDs, although *ab initio* DFT calculations demonstrated that C_iO_iH rings and multi (n) oxygen-involved C_iO_nH rings had shallow donor states.[22,23]

Based on the obtained results, the intensities of the *X* lines and the integrated HD concentrations in the m:Cz and FZ samples are displayed as a function of the annealing temperature in Fig. 8. The formation and decay of both the HDs and the *X* center occurred approximately over a temperature range of 260–520 °C. We particularly focus on the correlation of the decay temperature of the HDs with that of the *X* center. Figure 8 shows that the decay temperature of the *X* center (460–540 °C) has a strong correlation with that of the HD with higher thermal stability. In early studies investigating proton-irradiation-induced HDs, Gorelkinskii *et al.*[16] suggested that interstitial Si clusters participated in the HD formation process, based on the discussion about stress-induced reorientation energy of HDs. Tokmoldin and Mukashev[18,19] reported Si–H bond stretching modes originating from interstitial silicon clusters attached to hydrogen and correlated it with HDs. Therefore, based on the similarity of the decay temperature, we tentatively interpret

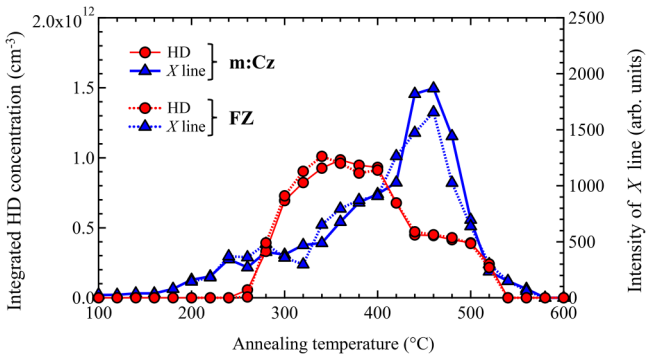

FIG. 8. Intensity of the *X* line and the integrated HD concentration as a function of the annealing temperature observed in m:Cz and FZ samples. The solid and dotted lines are shown solely to facilitate visualization for the m:Cz and FZ samples, respectively.

Published under an exclusive license by AIP Publishing

that the HD with higher thermal stability is defect complexes consisting of the *X* center partially passivated with hydrogen: the dissociation of the core defect (*X* center) dominates the disappearance of the donor states of the HD because the Si–H bond is stable at 600 °C.[43]

Although a strong correlation between the formation and the decay temperatures of the *X* and HD centers was observed, the defects that have a decay temperature similar to the HD with lower thermal stability are missing, probably because the corresponding defects are optically inactive. The formation and decay temperatures of the 1114-meV lines were also uncorrelated with those of the HDs. Further studies using the techniques such as EPR are essential to clarify the origin of the HD that is less thermally stable.

IV. CONCLUSIONS

Proton-irradiation-induced HDs and luminescent defects were investigated in *n*-type m:Cz and FZ silicon wafers as a function of annealing temperature. HD formation occurred at 260 °C, and its concentration decreased in two stages at 400–440 °C and 500–540 °C, indicating the existence of two types of HDs with different thermal stabilities. PL measurements showed the generation of the interstitial silicon-related *W* and *X* centers, *C* center, and exciton lines bound to unknown shallow centers depending on the annealing temperature. The fact that the thermal process is essential for the formation of HDs suggests that the core defects of HDs are generated during the annealing stage. This fact ruled out the incorporation of predominant defects at low-temperature annealing, such as C_iO_i and the *W* center, into the core of HDs. In contrast, the *X* center was generated at a temperature above 200 °C and disappeared at 580 °C. These temperatures were comparable to the formation and decay temperatures of HD with higher thermal stability. The similarity of the formation and decay temperatures between the *X* center and the HD suggests that the HD is associated with the interstitial silicon-related defects attached to hydrogen. However, further investigation using techniques such as EPR is necessary to definitively determine the relationship between HDs and interstitial Si and identify the defect responsible for the HD with lower thermal stability. An investigation of the defect formation with different doses and energies of proton irradiation is also the subject of a future study. The findings of this study provide an understanding of the underlying physical mechanism of the proton-irradiation doping process to fabricate modern power devices and facilitate the progress of hydrogen-related silicon technology.

ACKNOWLEDGMENTS

The authors would like to thank J. Ito (SHI-ATEX Co., Ltd) and S. Takemoto (Melco Semiconductor Engineering Corp.) for their assistance with the proton-irradiation experiments and spreading resistance profiling measurements, respectively. The authors would also like to thank Y. Kamiura (Professor Emeritus of Okayama University) for the helpful discussions and critical review of this manuscript.

AUTHOR DECLARATIONS

Conflict of Interest

The authors have no conflicts to disclose.

Ethics Approval

Ethics approval is not required.

DATA AVAILABILITY

The data that support the findings of this study are available within the article.

REFERENCES

[1] Y. Zohta, Y. Ohmura, and M. Kanazawa, Jpn. J. Appl. Phys. **10**, 532 (1971).
[2] Y. Gorelkinskii and N. N. Nevinnyi, Nucl. Instrum. Methods Phys. Res., Sect. A **209–210**, 677 (1983).
[3] H. J. Schulze, H. Öfner, F.-J. Niedernostheide, J. G. Laven, H. P. Felsl, S. Voss, A. Schwagmann, M. Jelinek, N. Ganagona, A. Susiti, T. Wübben, W. Schustereder, A. Breymesser, M. Stadtmüller, A. Schulz, T. Kurz, and F. Lükermann, in *Proceedings of the 28th International Symposium on Power Semiconductor Devices & ICs (ISPSD), Prague, Czech Republic* (IEEE, 2016), p. 355.
[4] M. Nemoto, T. Yoshimura, and H. Nakazawa, Appl. Phys. Express **1**, 051404 (2008).
[5] K. Nakamura, S. Nishizawa, and A. Furukawa, IEEE Trans. Electron Devices **67**, 2437 (2020).
[6] J. Hartung and J. Weber, Phys. Rev. B **48**, 14161 (1993).
[7] V. P. Markevich, M. Suezawa, K. Sumino, and L. I. Murin, J. Appl. Phys. **76**, 7347 (1994).
[8] V. P. Markevich, M. Suezawa, and L. I. Murin, J. Appl. Phys. **84**, 1246 (1998).
[9] H. Hatakeyama and M. Suezawa, J. Appl. Phys. **82**, 4945 (1997).
[10] R. Job, F.-J. Niedernostheide, H.-J. Schulze, and H. Schulze, MRS Proc. **1108**, 120 (2008).
[11] J. G. Laven, R. Job, W. Schustereder, H.-J. Schulze, F.-J. Niedernostheide, H. Schulze, and L. Frey, Solid State Phenom. **178–179**, 375 (2011).
[12] R. Job, J. G. Laven, F.-J. Niedernostheide, H.-J. Schulze, H. Schulze, and W. Schustereder, Phys. Status Solidi A **209**, 1940 (2012).
[13] J. G. Laven, R. Job, H.-J. Schulze, F.-J. Niedernostheide, W. Schustereder, and L. Frey, ECS J. Solid State Sci. Technol. **2**, P389 (2013).
[14] J. Hartung and J. Weber, J. Appl. Phys. **77**, 118 (1995).
[15] Y. Tokuda, A. Ito, and H. Ohshima, Semicond. Sci. Technol. **13**, 194 (1998).
[16] Y. V. Gorelkinskii, N. N. Nevinnyi, and K. A. Abdullin, J. Appl. Phys. **84**, 4847 (1998).
[17] E. Ntsoenzok, P. Desgardin, M. Saillard, J. Vernois, and J. F. Barbot, J. Appl. Phys. **79**, 8274 (1996).
[18] S. Z. Tokmoldin and B. N. Mukashev, Mater. Sci. Forum **258–263**, 223 (1997).
[19] S. Z. Tokmoldin and B. N. Mukashev, Phys. Status Solidi B **210**, 307 (1998).
[20] A. Kiyoi, N. Kawabata, K. Nakamura, and Y. Fujiwara, J. Appl. Phys. **129**, 025701 (2021).
[21] A. Kiyoi, N. Kawabata, K. Nakamura, and Y. Fujiwara, J. Appl. Phys. **130**, 115704 (2021).
[22] J. Coutinho, R. Jones, P. R. Briddon, S. Öberg, L. I. Murin, V. P. Markevich, and J. L. Lindström, Phys. Rev. B **65**, 014109 (2001).
[23] C. P. Ewels, R. Jones, S. Öberg, J. Miro, and P. Deák, Phys. Rev. Lett. **77**, 865 (1996).
[24] J. F. Ziegler, J. P. Biersack, and U. Littmark, in *The Stopping and Range of Ions in Solids*, Stopping and Ranges of Ions in Matter Vol. 1 (Pergamon Press, New York, 1984).
[25] S. J. Pearton, J. W. Corbett, and T. Shi, Appl. Phys. A **43**, 153 (1987).

Published under an exclusive license by AIP Publishing

[26]G. Davies and R. C. Newman, in *Handbook on Semiconductors*, edited by T. S. Moss, and S. Mahajan (Elsevier, Amsterdam, 1994), Vol. 3, p. 1557.
[27]R. Jones and S. Öberg, Phys. Rev. Lett. **68**, 86 (1992).
[28]P. M. Mooney, L. J. Cheng, M. Süli, J. D. Gerson, and J. W. Corbett, Phys. Rev. B **15**, 3836 (1977).
[29]M. Suezawa, N. Fukata, Y. Iijima, and I. Yonenaga, Jpn. J. Appl. Phys. **53**, 091302 (2014).
[30]G. Davies, E. C. Lightowlers, and Z. E. Ciechanowska, J. Phys. C: Solid State Phys. **20**, 191 (1987).
[31]M. Nakamura and S. Nagai, Phys. Rev. B **66**, 155204 (2002).
[32]P. K. Giri, Semicond. Sci. Technol. **20**, 638 (2005).
[33]A. Carvalho, R. Jones, J. Coutinho, and P. R. Briddon, Phys. Rev. B **72**, 155208 (2005).
[34]B. J. Coomer, J. P. Goss, R. Jones, S. Öberg, and P. R. Briddon, Phys. B: Condens. Matter **273–274**, 505 (1999).
[35]R. Jones, T. A. G. Eberlein, N. Pinho, B. J. Coomer, J. P. Goss, P. R. Briddon, and S. Öberg, Nucl. Instrum. Methods Phys. Res., Sect. B **186**, 10 (2002).
[36]G. Davies, S. Hayama, L. Murin, R. Krause-Rehberg, V. Bondarenko, A. Sengupta, C. Davia, and A. Karpenko, Phys. Rev. B **73**, 165202 (2006).
[37]D. Pierreux and A. Stesmans, Phys. Rev. B **71**, 115204 (2005).
[38]B. N. Mukashev, A. V. Spitsyn, N. Fukuoka, and H. Saito, Jpn. J. Appl. Phys. **21**, 399 (1982).
[39]A. N. Safonov and E. C. Lightowlers, Mater. Sci. Eng., B **58**, 39 (1999).
[40]A. S. Kaminskii, E. V. Lavrov, G. Davies, E. C. Lightowlers, and A. N. Safonov, Semicond. Sci. Technol. **11**, 1796 (1996).
[41]R. Sauer and J. Weber, Physica B+C **116**, 195 (1983).
[42]B. Hourahine, R. Jones, A. N. Safnov, S. Oberg, P. R. Briddon, and S. K. Estreicher, Phys. Rev. B **61**(12), 2594 (2000).
[43]H. J. Stein, J. Mater. Sci.: Mater. Electron. **4**, 159 (1975).

Published under an exclusive license by AIP Publishing